J Appl Electrochem (2012) 42:935–943
DOI 10.1007/s10800-012-0469-2

ORIGINAL PAPER

Chitosan hydrogel-based electrode binder and electrolyte membrane for EDLCs: experimental studies and model validation

Nurul A. Choudhury · Paul W. C. Northrop · Andrew C. Crothers · Shruti Jain · Venkat R. Subramanian

Received: 5 June 2012 / Accepted: 31 July 2012 / Published online: 19 August 2012

Abstract Experimental studies and model validation thereof on all solid-state electrical double layer capacitors (EDLCs) comprising of a novel, cost-effective, and eco-friendly electrode binder consisting of chitosan chemical hydrogel (CCH), and a separator consisting of ionically cross-linked chitosan hydrogel membrane electrolyte (IC-CSHME) are reported. The EDLCs have been assembled with black pearls carbon as electrode. The ICCSHME has been prepared by ionic cross-linking of chitosan (CS) with sodium sulfate. EDLCs comprising 40 % loading of CCH electrode binder and ICCSHME with 1 M NaOH dopant have been studied by galvanostatic chronopotentiometry. The data have been analyzed using mathematical modeling to study lifetime behavior of the EDLCs.

Keywords Chitosan · Chemical hydrogel · Electrode binder · Electrical double layer capacitor · Modeling

1 Introduction

EDLCs are electrochemical power systems with highly reversible charge storage and delivery capabilities. EDLCs have properties complementary to secondary batteries and find use in hybrid energy systems for electric vehicles, heavy-load starting assist for diesel locomotives, utility load leveling, military and medical applications [1, 2]. The higher energy density of EDLCs as compared to dielectric capacitors is primarily due to the large surface area and porosity of the electrode materials, usually comprising of activated carbons [3, 4], aerogel or xerogel carbons, [3, 5–7] or carbon nanotubes [3, 8, 9]. EDLCs have several advantages over secondary batteries, namely faster charge–discharge, longer cycle-life ($>10^5$ cycles) and higher power density [1]. EDLCs employ both aqueous and non-aqueous electrolytes in either liquid or solid state; the latter provides advantages of compactness, reliability and freedom from leakage of liquid.

Hydrogels are 3-dimensional solid polymeric networks that absorb and retain many times their dry weight of water within their polymeric matrices. Chemical hydrogels are formed by a chemical reaction between a polymer and a cross-linking reagent [10]. Polymer hydrogels have been used as solid electrolytes in electrochemical devices [11–13]. PVA and gelatin chemical hydrogels have been reported as solid electrolytes in supercapacitors [12, 14]. Choudhury et al. [15] reviewed various polymer hydrogel electrolytes for application in supercapacitors.

CS is a natural polymer that is derived by deacetylation of chitin [poly (*N*-acetyl-D-glucosamine)]. Chitin, which is present in the exoskeleton of arthropods, is the second most abundant natural polymer after cellulose [16]. CS is weakly alkaline and is soluble in dilute aqueous solution of a weak acid such as lactic acid, acetic acid (CH_3COOH) etc. that converts the glucosamine unit ($R–NH_2$) of CS into its protonated form ($R–NH_3^+$). Being inexpensive, biodegradable, and nontoxic, CS finds use as an additive in food industry, as a hydrating agent in cosmetics, and as a pharmaceutical agent in medicine [17]. A polymer electrolyte membrane (PEM) comprising CS as matrix and KOH as dopant exhibited ionic conductivity in order of 10^{-2} S cm^{-1}. A PEFC employing the CS–KOH composite

N. A. Choudhury · P. W. C. Northrop · A. C. Crothers · S. Jain · V. R. Subramanian (✉)
Department of Energy, Environmental, and Chemical Engineering, Washington University, One Brookings Drive, St. Louis, MO 63130, USA
e-mail: vsubramanian@seas.wustl.edu

as PEM, platinum as both anode and cathode catalysts, hydrogen as fuel, and air as oxidant delivered a current density of 30 mA cm^{-2} [18]. CS hydrogel can be prepared by either chemical cross-linking of CS with aldehydes such as glutaraldehyde or ionic cross-linking of CS with polyatomic multivalent anions such as sulfate ion, phosphate ion etc. The chemical cross-linking reaction between CS and glutaraldehyde takes place by Schiff base mechanism [19]. Rohindra et al. [20] reported that for CCH, equilibrium swelling ratio (E_{sr}) in an aqueous medium that is inversely related to its mechanical strength decreased with increase in the extent of chemical cross-linking and pH of the aqueous media but increased with increase in both time and temperature. Ionic interaction between CS and H_2SO_4 was studied by Cui et al. [21]. CS hydrogel membrane prepared by ionic cross-linking of CS with H_2SO_4 was employed as electrolyte-cum-separator in DMFC by Osifo et al. [22]. Use of H_2SO_4 as cross-linking agent is accompanied by health hazard. Moreover, handling and use of H_2SO_4, a corrosive liquid reagent, as cross-linking agent is cost-intensive. Use of salts such as sodium sulfate overcomes both of these limitations. Du et al. [23, 24] have reported studies on preparation, structure, and proton conductivity of CS membranes doped with ammonium acetate, ammonium chloride, and ammonium sulfate. Choudhury et al. [25] reported studies on various characterizations of ICCSHMEs prepared by ionic cross-linking of CS with sodium sulfate (Na_2SO_4) and sodium hydrogen phosphate as well as their performance evaluations as electrolyte-cum-separators in direct borohydride fuel cells (DBFCs).

There are a few more reports in literature on the use of CS in various modified forms as PEMs for fuel cells. CCH has been studied by Choudhury et al. [26, 27] as electrode binder in DBFCs. Nafion® has been studied as electrode binder as well as electrolyte membrane in EDLCs by Lufrano et al. [28, 29]. However, to the best of our knowledge, CCH has not been employed as electrode binder in EDLCs. Use of CCH as electrode binder and ICCSHME as separator provides some advantages to the EDLC such as cost-effectiveness, eco-friendliness, ease of handling resulting from solid-state nature of its electrolyte/separator, and high electrochemical performance resulting from high water retention capability of chitosan. Chitosan, the precursor of both CCH and ICCSHME, is derived from chitin that is the second most abundant polymer in nature [16] by a low-cost process. Moreover, preparation of CCH binder-based electrode and ICCSHME separator, as reported previously [25–27] and also described below in Sect. "2", is simple, inexpensive, and time-effective.

In order to analyze the behavior of EDLCs across a wide range of operating conditions and designs, computer simulations can be utilized. Using simulations allows for more scenarios to be examined than could be practically analyzed using experimental techniques. This requires using a model to describe the operation of EDLCs as a function of physical parameters and operating conditions. Using these models allows calculation of internal parameters that cannot be easily directly measured. Several models have been presented in the literature with varying degrees of details [30–37]. The simplest of such models describes the EDLCs as a system of ideal resistors and parallel plate capacitors arranged in various series and parallel combinations [30–32]. These have the advantage of allowing quick simulation and easy insertion into other circuit models to describe hybrid systems. However, these rely on several assumptions that limit the use of such models [32]. Srinivasan and Wiedner [33] developed a model to describe EDLCs by considering the solid and liquid potentials within the capacitor. They were able to analytically solve the potential profiles and overall voltage for galvonostatic discharge. Other researchers have included additional physical phenomena, such as ionic concentration in porous electrodes [34–36] or pseudo capacitance resulting from the occurrence of oxidation/reduction reactions [36, 37]. In this paper, we report our studies on the use of CCH as electrode binder in EDLCs. Additionally, the charge–discharge data recorded from the EDLCs have been analyzed using mathematical models.

2 Experimental details

2.1 Preparation of CS solution

A 2 % (w/v) aqueous solution of CS was prepared by adding the required amount of CS powder (MW: 100,000–300,000; Acros Organics) to a given volume of 2 % (v/v) aqueous solution of glacial acetic acid (Certified ACS reagent, Fisher Scientific) in a glass beaker. The beaker was covered with Parafilm so as to prevent evaporation of water and the contents were stirred magnetically at ambient temperature for ~12 h to obtain a pale yellow solution.

2.2 Preparation of ICCSHMEs

ICCSHMEs were prepared by a solution casting technique in which the required volume of 2 % (w/v) solution of CS, as prepared by a procedure described in Sect. 2.1, was cast on a polystyrene Petri dish and left at ambient conditions of temperature and pressure for ~36 h to allow the water to evaporate. After the aforesaid period, the solid layer of CS peeled off automatically. A sufficient volume of 0.5 M aqueous solution of sodium sulfate ($Na_2SO_4 \cdot 10H_2O$, Fisher Chemical) was then added to the Petri dish so as to completely dip the dried CS film inside the salt solution. The Petri dish was covered with a piece of Parafilm so as to

prevent evaporation of water from salt solution and left at ambient temperature for about 24 h to allow absorption of salt solution by the dried CS film. The negatively charged sulfate ions (SO_4^{2-}) absorbed in the wetted CS film form ionic crosslinks with positively charged ammonium ion moiety ($-NH_3^+$) of CS. Due to the absorption of salt solution and subsequent ionic cross-linking, the CS film turns into a hydrogel film that is insoluble in water and aqueous solutions. The ICCSHME was then taken out of the salt solution bath, washed thoroughly with DI water, and stored in de-ionized water (DI) water bath for use in EDLCs.

2.3 Preparation of CCH binder-based electrode

The electrode material employed in this study was Black Pearls Carbon (BPC). In order to prepare electrode ink, a certain amount of BPC powder (Cabot Corporation, Boston, MA, USA) was mixed with adequate quantity of methanol solvent in a glass vial using a magnetic stirrer for 2 h. Subsequently, the required volume of CCH binder [26, 27] solution, comprising 0.5 % (w/v) solution of CS dissolved in 2 % (v/v) aqueous CH_3COOH solution, was added dropwise to the aforesaid suspension with mixing continued for another 2 h. The loading of BPC was 0.9 mg cm^{-2}. The electrode ink was coated on Toray Carbon paper (TGPH-060) substrate, and the electrode ink-coated Toray Carbon paper was dried at ambient temperature for 12 h, weighed to determine electrode loading, and then dipped in 10 mL of 6.25 % (v/v) aqueous glutaraldehyde solution for 5 h to cause the cross-linking reaction between CS and glutaraldehyde to occur. After the treatment, the electrode-coated Toray Carbon paper was washed thoroughly with DI water to remove excess impurities. Methanol was chosen as the solvent for preparing electrode ink because it is hydrophilic and polar enough to mix with the water-based electrode binder solution and volatile enough to facilitate fast drying at ambient temperature of the electrode ink after its coating on the Toray carbon paper electrode substrate.

2.4 Electrochemical characterizations of EDLCs

For the electrochemical performance characterization of EDLCs, membrane electrode assemblies (MEAs) were fabricated by sandwiching two identical electrodes on either side of an ICCSHME. The two electrodes of each of the MEAs were contacted on their rear with two copper current collectors embedded in Teflon holders. The active area of each of the electrodes was 2.25 cm^2. After installing the EDLCs in the test station, performance evaluation studies were initiated. The charge/discharge data were recorded at a constant current value of 1 mA in the potential range between 0.1 and 1.0 V by employing a computer-controlled automated battery tester (Arbin Instruments).

Table 1 Dimensionless variables used in EDLC model

I^*_{Eff}	$\frac{I_{\mathrm{app}}L(\kappa+\sigma)F}{\kappa\sigma RTA}$
τ	$\frac{t\kappa\sigma}{aCL^2(\kappa+\sigma)}$
β	$\frac{R_s\kappa\sigma}{L(\kappa+\sigma)}$
γ	$\frac{\kappa}{\sigma}$
V^*	$2V_0$

2.5 Mathematical model

A mathematical model was used to describe the behavior of the EDLCs and estimate the physical parameters characterizing the system. The model was based on the analytical solution presented by Srinivasan and Wiedner [33] with minor adjustments to account for current leakage in a manner similar to that given by Diab et al. [30]. In dimensionless form, the voltage can be predicted from Ref. [33] as for constant current discharge:

$$V^* = V_0^* - I^*_{\mathrm{Eff}}\left[\frac{1}{3}+\tau-2\sum_{n=1}^{\infty}\frac{\left(\frac{(-1)^n\gamma+1}{\gamma+1}\right)^2\exp(-n^2\pi^2\tau)}{n^2\pi^2}-\frac{\beta}{2}\right] \quad (1)$$

This model can be verified using experimental data and allows for estimation of the important physical parameters for electrochemical operation. A full list of the dimensionless variables used in this paper is given in Table 1.

Parameter estimation was performed using the built-in MATLAB function "lsqnonlin" to minimize the sum of the squares of the residuals of the experimental data relative to the model prediction. Similar approaches have been used in the past for estimating parameters and modeling capacity fade of lithium-ion batteries [38–41]. Wherever possible, parameters were determined a priori by experimental design or as material properties determined from the literature. This left two parameters to be determined from experimental data: the specific capacitance aC, (F/cm^3) and the separator resistance, R_s, (Ω). The specific capacitance is actually a combination of two parameters: the particle surface area per volume, a (cm^2/cm^3), and the capacitance per interfacial area, C (F/cm^2), that cannot be estimated independently. Overall, the specific capacitance represents the amount of charge that can be stored per unit volume of the electrode. This can be affected by the size of the particles used, or the type of material used. Adding a dopant may also help to stabilize the electrical double layer, thereby increasing the available capacitance.

The separator resistance, R_s, incorporates the resistance due to the membrane properties and conditions, as well as any contact resistance between the membrane and electrode. This has the effect of causing an immediate voltage drop at the beginning of discharge, and a voltage rise at the beginning of charge with the ultimate consequence of decrease in the amount of charge that can be stored.

In order to better capture the dynamical behavior of the EDLC, a three-parameter model was developed as a modification to the above model. This was done by considering leakage current that occurs across the EDLC. The leakage current was modeled as an equivalent resistor in parallel with the EDLC. Examples of this mechanism being applied to model and simulate self-discharge can be found in the literature [30]. The inclusion of current leakage in this manner results in an additional discharge current proportional to the voltage of the EDLC. In the case of an EDLC undergoing relaxation (i.e., not charging or discharging), this would result in an exponential decrease in voltage due to the self-discharge. However, during charging and discharging, the current leakage has the effect of modifying the effective applied current. Since this mechanism is strictly discharging in nature, a greater effective current is seen during discharge while a lesser current is applied during charging, creating an asymmetry between the charging and discharging cycles, which is observed experimentally. Mathematically, this is represented as:

$$I^*_{\mathrm{Eff}} = I^*_{\mathrm{Act}} + \epsilon V^* \tag{2}$$

By inserting 2 into 1, and solving for V^* we arrive at:

$$V^* = \frac{V^*_0 - I^*_{\mathrm{Act}}\left[\frac{1}{3} + \tau - 2\sum_{n=1}^{\infty}\frac{\left(\frac{(-1)^n\gamma+1}{\gamma+1}\right)^2\exp(-n^2\pi^2\tau)}{n^2\pi^2} - \frac{\beta}{2}\right]}{1 + \epsilon\left[\frac{1}{3} + \tau - 2\sum_{n=1}^{\infty}\frac{\left(\frac{(-1)^n\gamma+1}{\gamma+1}\right)^2\exp(-n^2\pi^2\tau)}{n^2\pi^2} - \frac{\beta}{2}\right]} \tag{3}$$

This introduces an additional parameter to the model that must be estimated. This leakage parameter, ϵ (S), is equivalent to $\frac{1}{R^*_{\mathrm{Leak}}}$. The leakage parameter, ϵ, represents any mechanism which causes self-discharge of the capacitor, which is proportional to voltage. This parameter causes the capacitor to discharge faster at the early stages of discharge, and increases the non-linear nature of the discharge curve.

3 Results and discussion

A comparative study of CCH, Polyvinyl alcohol chemical hydrogel (PCH), and Nafion® as electrode binders in fuel cell was previously reported by one of the authors [27]. It was observed that CCH binder exhibited better performance as compared to both PCH and Nafion® binders. The better performance of CCH was ascribed to its greater hydrophilic nature and consequent greater water retention capability as compared to those of PCH and Nafion® binders. Because of the superior performance in fuel cells, chitosan-based hydrogels have been used as electrode binder and electrolyte separator in EDLCs in this study. Greater water retention capability of chitosan helps in effective formation and better stabilization of double electric layer at the electrode/electrolyte interface, thereby enhancing the capacitive properties of the EDLC. Chitosan was chosen as the polymeric material for EDLC in this study because of its good performance as electrode binder [26, 27] and electrolyte membrane [25] in fuel cells. The chemical reaction that occurs between CS and acetic acid in aqueous medium is shown in Fig. 1. The main functional group present in each monomer unit of CS is the amine group ($–NH_2$), and the remaining structural moiety is represented by R that comprises a six-membered ring structure, which in turn contains an ether group and a primary alcohol group attached to its backbone [42]. This reaction results in the protonation of $–NH_2$ group of CS and is responsible for dissolution of CS in aqueous acetic acid medium. CS, dissolved in aqueous CH_3COOH solution, undergoes a chemical cross-linking reaction with aqueous glutaraldehyde at ambient temperature and pressure. Due to the reaction, aqueous solution of CS becomes a solid mass with all water associated with the precursor solutions remaining absorbed in the polymer matrix of the solid entity. Such a solid entity is referred to as chitosan chemical hydrogel. During solidification of aqueous solutions of CS and glutaraldehyde in the presence of electrode materials, the electrode materials get bonded with one another and also to the electrode substrate. The large quantity of water absorbed in the CS hydrogel matrix during electrode fabrication helps in the formation of efficient electrical double layer and hence in achieving high electrochemical performance of the EDLCs. CCH is insoluble in water and does not disintegrate on heating. These characteristics make CCH a suitable electrode binder

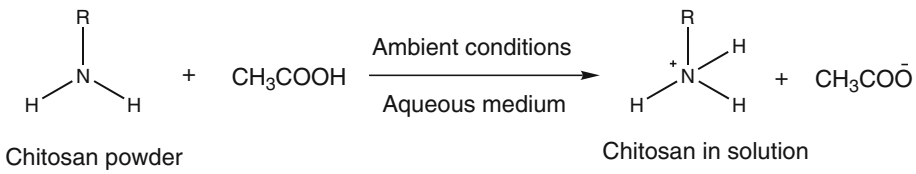

Fig. 1 Chemical reaction between chitosan and acetic acid in aqueous medium

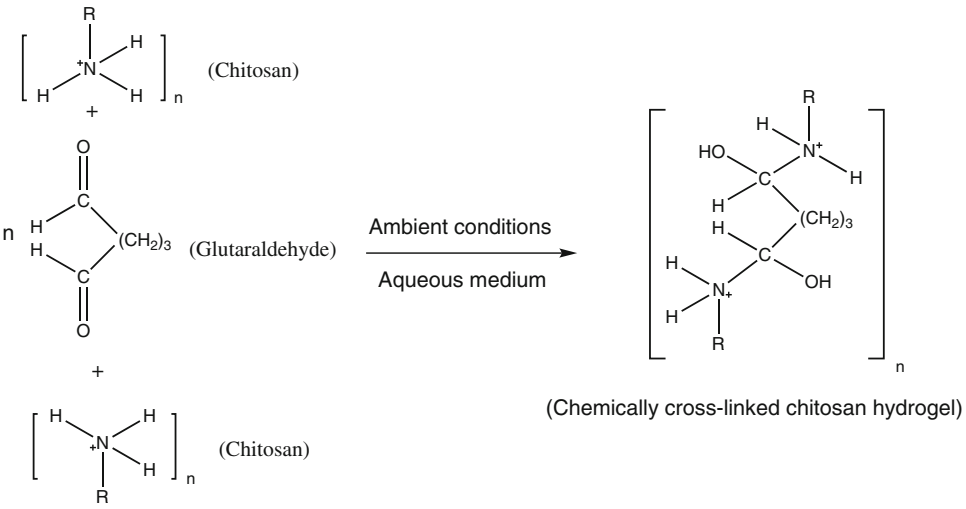

Fig. 2 Chemical reaction between protonated chitosan and glutaraldehyde in aqueous medium leading to the formation of chitosan chemical hydrogel binder

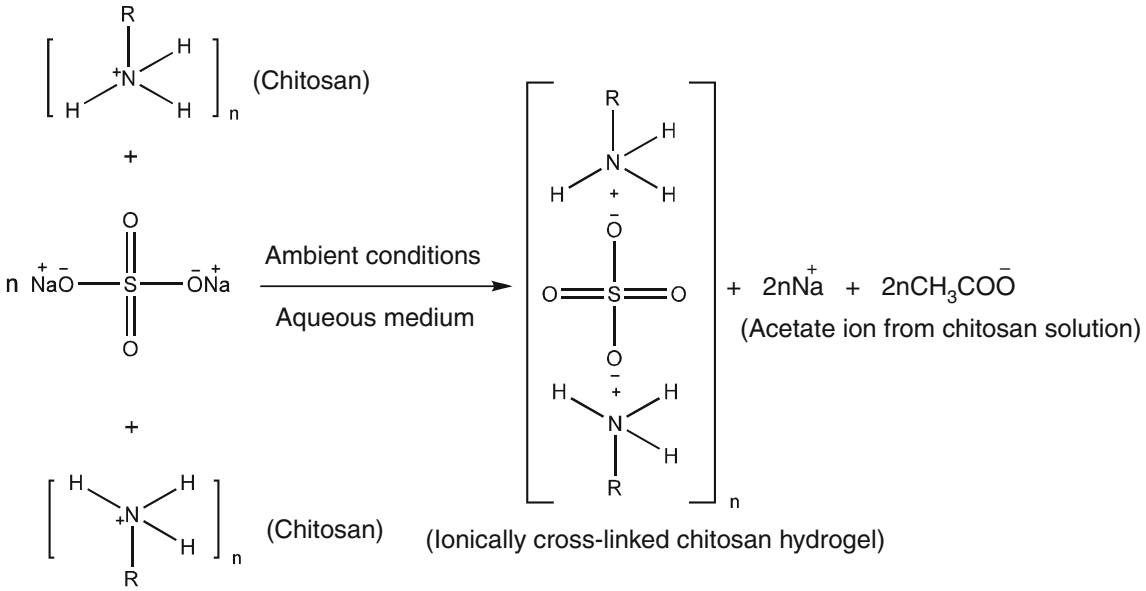

Fig. 3 Ionic interaction between protonated chitosan and sulfate ion in aqueous medium leading to the formation of ionically cross-linked chitosan hydrogel membrane electrolyte

for additional applications in EDLCs with liquid electrolytes and at elevated operating temperatures. The chemical reaction between protonated CS and glutaraldehyde in aqueous medium leading to the formation of chitosan chemical hydrogel is shown in Fig. 2.

CS, dissolved in aqueous CH_3COOH solution, behaves as a polycation with $–NH_3^+$ groups attached to its backbone. Two positively charged $–NH_3^+$ groups of one or two CS polycation chains form two ionic bonds with two negatively charged oxygen moieties of one sulfate ion at ambient temperature and pressure. This type of ionic bond formation takes place at multiple sites of CS polycation chains. Due to the ionic cross-linking process, CS film turns into a water-insoluble hydrogel film. Such a hydrogel film contains a number of mobile ionic species [25] that are capable of carrying ionic charge between electrodes and is referred to as ionically cross-linked CS hydrogel membrane electrolyte (ICCSHME). Ionic interaction between protonated CS and sulfate ion in aqueous medium leading to the formation of ICCSHME is shown in Fig. 3.

The EDLC was cycled between constant current charging and constant current discharging until failure. Figure 4 shows the full charge–discharge profiles for a representative sample of cycles throughout the life of the capacitor. Notice that there is very little change between the profiles for cycle 20 and cycle 200. This suggests that the capacitor is stable during operation between these cycles. However, significant fade can be noticed by cycle 500; by cycle 1400, the capacitor is effectively dead (Table 2).

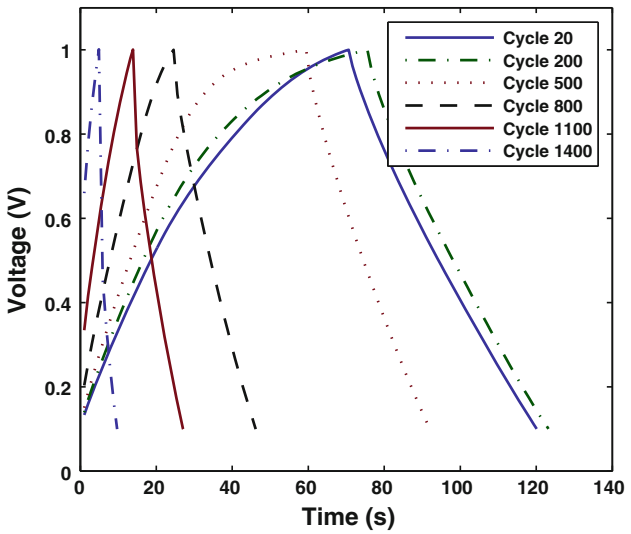

Fig. 4 Charge/discharge plots for several cycles in the life of the EDLC

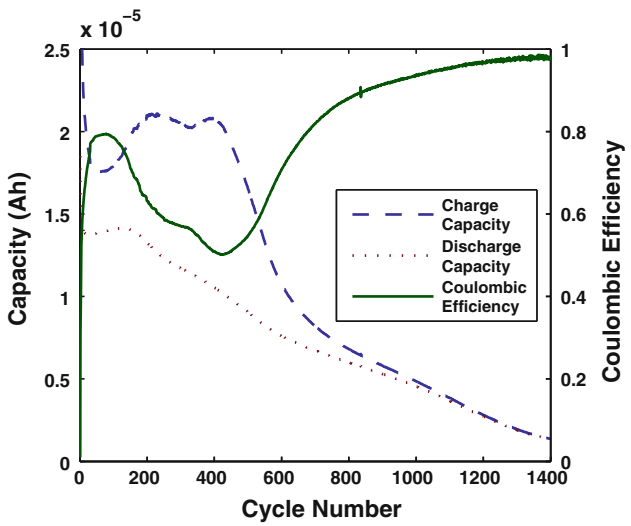

Fig. 5 Charge capacity (*dashed line*), discharge capacity (*dotted line*), and coulombic efficiency (*solid line*, *right axis*) for the life of the EDLC

Table 2 Design and known parameters

L	Electrode thickness	60×10^{-4} cm
σ	Solid phase conductivity	100 S
κ	Electrolyte conductivity[a]	1×10^{-4} S/cm^2
A	Electrode cross-sectional area	2 cm^2
I_{app}	Applied current	0.001 A

[a] From Ref. [16]

Parameter estimation was performed for both the two-parameter model given in Eq. 2 and the three-parameter model given in Eq. 3. Graphically, Fig. 5 shows the discharge profiles for several cycles across the life of the electrode, as well as the two- and three-parameter model fits for the same cycles. Qualitatively, the three-parameter model fits the data better, as would be expected when more parameters are considered. In order to verify that including the leakage parameter statistically improves the model, an F test was performed. These results are shown in Table 3 for several cycles. The F-condition value in the last column of Table 3 represents a 95 % probability that the inclusion of the leakage parameter is justified. Note that the F value is much greater than the condition value for each cycle analyzed, which shows that including the leakage parameter significantly improves the model.

Due to the statistically significant improvement of the three-parameter model over the two-parameter model, the remainder of the analysis will focus strictly on the three-parameter model. Table 4 shows the estimated parameters associated with these same cycles, as well as the 95 % confidence intervals. This clearly shows that capacity fade occurs during the life of the capacitor. Furthermore, it shows that the model can provide a good fit at all these cycles. Also, note that minimal capacity fade is observed during the first couple hundred cycles.

This is more clearly shown in Fig. 6, which shows the amount of capacity observed as a function of cycle number for both charging and discharging. This shows that the discharge capacity remains largely constant for the first 200 cycles, and then begins to fade in a regular pattern. The charging capacity does not follow as a clear trend, but begins to decrease monotonically after approximately cycle number 500. The Columbic efficiency is also shown on the

Table 3 F test to validating the inclusion of the leakage parameter

Cycle	Degrees of freedom	Residual norm—2 parameters (R_2)	Residual norm—3 parameters (R_3)	Variance—2 parameters	Variance—3 parameters	F value	95 % F-condition
20	49	0.0145	7.79e-4	3.09e-3	1.69e-5	8,516	4.05
200	48	0.0146	1.07e-3	3.17e-4	2.38e-5	569	4.05
500	33	0.0126	1.85e-4	4.06e-4	6.17e-6	2,013	4.17
800	22	7.30e-3	4.82e-5	3.65e-4	2.54e-6	2,859	4.38
1,100	14	4.86e-3	8.01e-5	4.05e-4	7.28e-6	656	4.84
1,400	5	6.83e-4	2.60e-6	2.28e-4	1.30e-6	523	18.512

Table 4 Estimated parameter values with 95 % confidence intervals as determined by simultaneously considering all experimental discharge cycles

Cycle	aC (F/cm^3)			R_s (Ω)			ε (S) (×10^4)		
	Low 95 %	Estimated value	High 95 %	Low 95 %	Estimated value	High 95 %	Low 95 %	Estimated value	High 95 %
20	4.911	4.941	4.972	53.983	69.320	89.014	3.383	3.674	3.990
200	4.755	4.789	4.823	84.572	103.436	126.503	3.314	3.656	4.032
500	3.258	3.273	3.287	80.905	93.516	108.092	4.055	4.282	4.522
800	2.213	2.221	2.229	169.093	180.108	191.840	4.029	4.221	4.422
1,100	1.554	1.569	1.584	549.659	577.943	607.684	5.394	5.989	6.649
1,400	0.869	0.889	0.910	1466.3	1536.6	1610.2	9.451	12.121	15.546

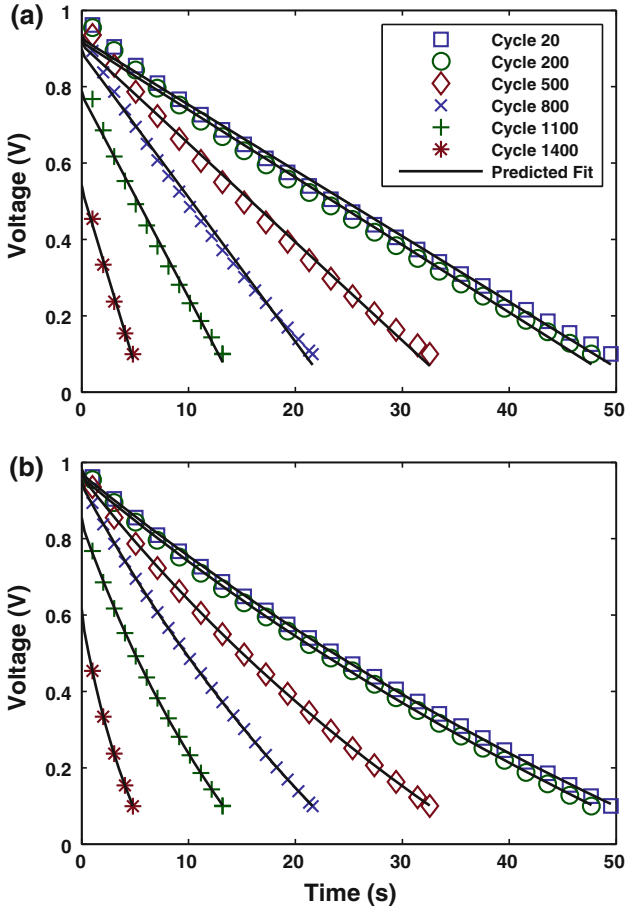

Fig. 6 Experimental discharge curves for several representative cycles, with model predicted curves from the parameter estimation analysis (*solid line*) using **a** two-parameter model, and **b** three-parameter model

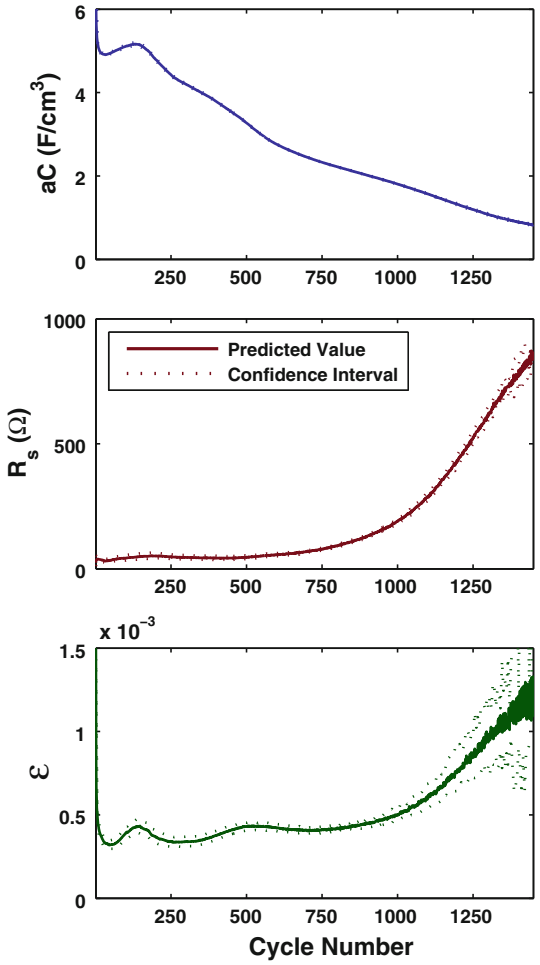

Fig. 7 Predicted parameter values as a function of cycle number (*solid lines*) as well as 95 % confidence intervals (*dashed lines*)

right axis of Fig. 6. The observed behavior suggests that the charging half of the full cycle is the dominant factor in determining the Columbic efficiency. Interestingly, the efficiency approaches unity as the capacitor approaches the end of life, though it is important to note that this is largely due to the relatively small amount of charge being stored.

For each cycle during the capacitor life, the following parameters were estimated: the specific capacitance (F/cm^3), the separator resistance, and the leakage parameter denoted by ϵ. The behavior of these parameters is shown in Fig. 7 for the life of the capacitor, while the 95 % confidence intervals of the parameter estimates are shown as dotted lines. This shows that the parameters are estimated

with good confidence, except for near the end of life for the separator resistance and leakage parameter. Furthermore, from approximately cycle 200 to cycle 800, the capacity fade is best represented by the specific capacitance, which decays in a manner which mirrors the fade of the capacity. This may suggest that the mechanism of capacity fade in this system involves degradation of the active material, as this would result in steeper discharge curve. This may be due to physical damage caused to the electrode, causing some of the carbon to no longer be electrically connected to the current collector, or due to reactions which occur at the carbon particles surface, reducing the surface area available for charge storage. Near the end of life, there is an increase observed in both the separator resistance as well as the leakage parameter. The larger separator resistance suggests some failing in the ICCSHME, or at the electrode/separator interface. The major reason for failing in ICCSHME could be due to the evaporation of water from it with the consequence of decrease in its ionic conductivity. Because of the evaporation of water, ICCSHME dries up and its contact with the electrode becomes inefficient with the result of increased electrode/ICCSHME interface resistance. This results in a significant drop in the open circuit voltage at the beginning of discharge, which can be clearly seen in Fig. 6. The leakage parameter also increases near the end of life in a manner similar to the ICCSHME separator resistance. This increases the curvature of the discharge curve as well as the rate of discharge. It is important to note that random variations were obtained in the estimated parameters and the observed capacity during the first 20 cycles, at which point they stabilize. We believe that this is due to the stabilization of the electrode during the first few cycles of operation.

MATLAB codes used for parameter estimation and capacity fade analysis as well as the experimental data and simulation files are available for public use on the corresponding author's website [43].

4 Conclusions

In this work, feasibility of using CCH and ICCSHME as novel, cost-effective, and environmentally benign electrode binder and polymer electrolyte membrane/separator, respectively, in EDLCs has been demonstrated. However, additional experiments would be required to compare the long- and short-term performances of EDLCs prepared with CCH and ICCSHME vis-à-vis EDLCs prepared with conventional materials. Preparations of CCH electrode binder and ICCSHME as well as assembling of EDLCs with such electrode binder and membrane electrolyte are simple and time-effective. The model proved an effective way of describing the capacity fade of the capacitor by estimating several physical parameters at each cycle. These parameters provide insight into the causes of the capacitor failure. The parameter estimation suggests that a decrease in capacitance occurs due to loss of available active material after the first couple hundred cycles of charges. As the capacitor approaches the end of life, the fade appears to be exasperated by the separator membrane degradation or dehydration leading to increased resistance and increased leakage. Attempts to simulate the charging portion of the cycle provided unsatisfactory fits, suggesting that there exists a mechanism that is unaccounted for in the model. Further analysis would be required to determine such a mechanism and an appropriate mathematical model to describe the asymmetry.

Acknowledgments The authors are thankful for the partial financial support of this work by the National Science Foundation (CBET-0828002, CBET-1008692, CBET-1004929), the United States government, McDonnell Academy Global Energy and Environment Partnership (MAGEEP) at Washington University in St. Louis.

References

1. Conway BE (1999) Electrochemical supercapacitors: scientific fundamentals and technological applications. Kluwer/Plenum, New York
2. Winter M, Brodd RJ (2004) Chem Rev 104:4245
3. Frackowiak E, Béguin F (2001) Carbon 39:937
4. Gamby J, Taberna PL, Simon P, Fauvarque JF, Chesneau M (2001) J Power Source 101:109
5. Mayer ST, Pekala RW, Kaschmitter JL (1993) J Electrochem Soc 140:446
6. Pekala RW, Farmer JC, Alviso CT, Tran TD, Mayer ST, Miller JM, Dunn B (1998) J Non Cryst Solids 225:74
7. Wang J, Zhang SQ, Guo YZ, Shen J, Attia SM, Zhou B, Zeng GZ, Gui YS (2001) J Electrochem Soc 148:D75
8. Frackowiak E, Meternier K, Bertagna V, Béguin F (2000) Appl Phys Lett 77:2421
9. Frackowiak E, Jurewicz K, Delpeux S, Béguin F (2001) J Power Sources 97–98:822
10. Kamath KR, Park K (1993) Adv Drug Deliv Rev 11:59
11. Panero S, Fiorenza P, Navarra MA, Romanowska J, Scrosati B (2005) J Electrochem Soc 152:A2400
12. Choudhury NA, Shukla AK, Sampath S, Pitchumani S (2006) J Electrochem Soc 153:A614
13. Sahu AK, Selvarani G, Pitchumani S, Sridhar P, Shukla AK, Narayanan N, Banerjee A, Chandrakumar N (2008) J Electrochem Soc 155:B686
14. Choudhury NA, Sampath S, Shukla AK (2008) J Electrochem Soc 155:A74
15. Choudhury NA, Sampath S, Shukla AK (2009) Energy Environ Sci 2:55
16. Wan Y, Creber KAM, Peppley B, Bui VT (2003) Polymer 44:1057
17. Qin C, Li H, Xiao Q, Liu Y, Zhu J, Du Y (2006) Carbohydr Polym 63:367
18. Wan Y, Peppley B, Creber KAM, Bui VT, Halliop E (2006) J Power Sources 162:105
19. Singh A, Narvi SS, Dutta PK, Pandey ND (2006) Bull Mater Sci 29:233

20. Rohindra DR, Nand AV, Khurma JR (2005) Polym Bull 54:195. http://www.publish.csiro.au/?act=view_file&file_id=SP04005.pdf
21. Cui Z, Xiang Y, Si J, Yang M, Zhang Q, Zhang T (2008) Carbohydr Polym 73:111
22. Osifo PO, Masala A (2010) J Power Sources 195:4915
23. Du JF, Bai Y, Chu WY, Qiao LJ (2010) J Polym Sci 48:260
24. Du JF, Bai Y, Chu WY, Qiao LJ (2010) J Polym Sci 48:880
25. Choudhury NA, Ma J, Sahai Y (2012) J Power Sources 210:358
26. Choudhury NA, Sahai Y, Buchheit RG (2011) Electrochem Commun 13:1
27. Choudhury NA, Ma J, Sahai Y, Buchheit RG (2011) J Power Sources 196:5817
28. Lufrano F, Staiti P, Minutoli M (2004) J Electrochem Soc 151:A64
29. Lufrano F, Staiti P (2004) Electrochim Acta 49:2683
30. Diab Y, Venet P, Gualous H, Rojat G (2009) IEEE Trans Power Electron 24:510
31. Shi L, Crow ML (2008) Power and energy society general meeting-conversion and delivery of electrical energy in the 21st century. IEEE, Pittsburgh
32. Nelms RM, Cahela DR, Tatarchuk BJ (2003) IEEE Trans Aerosp Electron Syst 39:430
33. Srinivasan V, Weidner JW (1999) J Electrochem Soc 146:1650
34. Sikha G, White RE, Popov BN (2005) J Electrochem Soc 152:A1682
35. Verbrugge MW, Liu P (2005) J Electrochem Soc 152:D79
36. Lin C, Popov BN, Ploehn HJ (2002) J Electrochem Soc 149:A167
37. Subramanian VR, Devan S, White RE (2004) J Power Sources 135:361
38. Ramadesigan V, Chen K, Burns NA, Boovaragavan V, Braatz RD, Subramanian VR (2011) J Electrochem Soc 158:A1048
39. Zhang Q, White RE (2008) J Power Sources 179:793
40. Stamps AT, Holland CE, White RE, Gatzke WP (2005) J Power Sources 150:229
41. Liaw BY, Jungst RG, Nagasubramanian F, Case HL, Doughty DH (2005) J Power Sources 140:157
42. Ma J, Choudhury NA, Sahai Y, Buchheit RG (2011) J Power Sources 196:8257
43. M.A.P.L.E Lab (2012) http://www.maple.eece.wustl.edu. Accessed 27 July 2012